11-1-2017

Imaging features of rare mesenychmal liver tumours: beyond haemangiomas.

Rajesh Thampy
University of Texas MD Anderson Cancer Center

Khaled M. Elsayes
University of Texas MD Anderson Cancer Center

Christine O. Menias
Mayo Clinic

Perry J. Pickhardt
University of Wisconsin-Madison

Hyunseon C. Kang
University of Texas MD Anderson Cancer Center

Follow this and additional works at: https://jdc.jefferson.edu/radiologyfp

See next page for additional authors

Part of the Radiology Commons

Let us know how access to this document benefits you

Recommended Citation

Authors

Rajesh Thampy, Khaled M. Elsayes, Christine O. Menias, Perry J. Pickhardt, Hyunseon C. Kang, Sandeep P. Deshmukh, Kareem Ahmed, and Brinda Rao Korivi

REVIEW ARTICLE

Imaging features of rare mesenychmal liver tumours: beyond haemangiomas

[1]RAJESH THAMPY, MD, [1]KHALED M ELSAYES, MD, [2]CHRISTINE O MENIAS, MD, [3]PERRY J PICKHARDT, MD, [1]HYUNSEON C KANG, MD, [4]SANDEEP P DESHMUKH, MD, [4]KAREEM AHMED, MD and [1]BRINDA RAO KORIVI, MD

[1]Department of Diagnostic Radiology, The University of Texas MD Anderson Cancer Center, Houston, TX, USA
[2]Department of Diagnostic Radiology, Mayo Clinic, Scottsdale, AZ, USA
[3]Department of Radiology, University of Wisconsin-Madison, Madison, WI, USA
[4]Department of Radiology, Thomas Jefferson University Hospital, Philadelphia, PA, USA

Address correspondence to: Khaled M Elsayes
E-mail: *Kmelsayes@mdanderson.org*

ABSTRACT

Tumours arising from mesenchymal tissue components such as vascular, fibrous and adipose tissue can manifest in the liver. Although histopathology is often necessary for definitive diagnosis, many of these lesions exhibit characteristic imaging features. The radiologist plays an important role in suggesting the diagnosis, which can direct appropriate immunohistochemical staining at histology. The aim of this review is to present clinical and imaging findings of a spectrum of mesenchymal liver tumours such as haemangioma, epithelioid haemangioendothelioma, lipoma, PEComa, angiosarcoma, inflammatory myofibroblastic tumour, solitary fibrous tumour, leiomyoma, leiomyosarcoma, Kaposi sarcoma, mesenchymal hamartoma, undifferentiated embryonal sarcoma, rhabdomyosarcoma and hepatic metastases. Knowledge of the characteristic features of these tumours will aid in guiding the radiologic diagnosis and appropriate patient management.

INTRODUCTION

Mesenchymal tumours are neoplasms that arise from vascular, fibrous, adipose, and other mesenchymal tissue components. Aside from haemangiomas, mesenchymal tumours are relatively uncommon in the liver. When they do arise within the liver, their appearance may mimic common malignant neoplasms. Hence, differentiation of these rare tumours from more common entities is relevant to clinical practice. Although histopathology is often necessary for definitive diagnosis, many of these lesions exhibit characteristic imaging features. The radiologist may be the first to suggest the diagnosis, which can direct appropriate immunohistochemical staining at histology. Recognition of these tumours can direct management with percutaneous tissue sampling rather than more invasive intervention. In some cases, identification of typical imaging findings may even prevent unnecessary biopsy. In this article, we review a spectrum of common and uncommon mesenchymal liver tumours and their imaging findings.

Haemangioma

Haemangiomas are the most common mesenchymal liver tumour, with a reported incidence of 1–6%.[1,2]

Histopathologically, haemangiomas are classified into three main subtypes: cavernous, capillary and sclerosing. Differentiating haemangiomas from other less common tumours is an issue often encountered in liver imaging, particularly with atypical forms of haemangiomas.

Cavernous haemangioma

The most common subtype, cavernous haemangiomas demonstrate a characteristic appearance on imaging. On ultrasound, cavernous haemangiomas typically appear as well-defined homogenous hyperechoic lesions with posterior acoustic enhancement. Dynamic CT/MR shows peripheral globular/nodular enhancement in arterial phase, with an attenuation of the enhancing portions similar to the aorta.[3] Progressive centripetal enhancement in the portal venous phase, and retention of contrast/"fill-in" on the delayed phase, are classic and also tend to follow blood pool.[4] On T_2 weighted MR images, they demonstrate high signal intensity, which slightly attenuates on longer TE T_2 weighted sequences, due to inherent vascular lakes and channels.[5] Overall, MRI has an accuracy exceeding 97%.[5,6]

A cavernous haemangioma greater than 5 cm is characterized as a giant haemangioma. This typically has a

heterogeneous appearance due to central thrombus, myxoid tissue or fibrosis.[7] On dynamic contrast CT/MRI, the typical early globular peripheral enhancement is present but complete filling is not seen. Its distinctive MRI appearance of high signal intensity on T_2 weighted images and discontinuous peripheral enhancement with enlargement and coalescence of the enhancing foci on serial post-contrast images aids in its diagnosis.[7] MR images may show a cleft-like area and sometimes internal septa, which demonstrate T1-hypointensity and T2-hyperintensity.[7]

Haemorrhage is a rare complication of cavernous haemangiomas, which may occur spontaneously or after anticoagulation therapy. Symptoms include acute epigastric pain and vomiting. The diagnosis is made when the typical enhancement pattern of haemangioma is combined with features suggestive of intratumoral haemorrhage, such as high attenuation on non-contrast CT and high signal on T_1 weighted images (Figure 1).

Capillary haemangioma
These constitute about 16% of all haemangiomas, and are typically seen in haemangiomas less than 1–2 cm in diameter—the "flash-filling" haemangioma.[8] Dynamic CT/MRI shows rapid enhancement on the arterial phase (roughly equivalent to the aorta) with contrast retention on the venous and delayed phases (Figure 2). This feature allows them to be differentiated from hypervascular tumours (*i.e.* HCC, hypervascular metastases) which typically demonstrate contrast wash-out on the delayed phase.[9]

Sclerosing haemangioma
Haemangiomas that exhibit degeneration and fibrous replacement are called sclerosed, thrombosed or hyalinized. Due to high fibrous content they lack the typical imaging features of a haemangioma, such as early peripheral enhancement, filling in on dynamic contrast CT/MRI and high signal intensity on T_2 weighted images. Therefore, the prospective diagnosis of sclerosing haemangioma can be difficult. However, a combination of findings such as transient hepatic attenuation difference

Figure 1. Haemorrhagic haemangioma: axial T_2 weighted image demonstrates a large well-circumscribed haemangioma within the right hepatic lobe with perilesional fluid compatible with subacute blood (arrows).
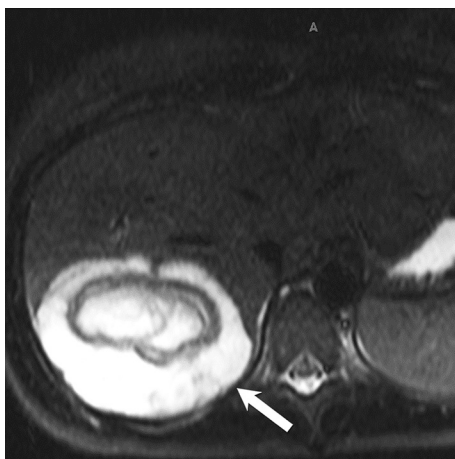

Figure 2. Flash-filling/capillary haemangioma: axial contrast-enhanced T_1 weighted images of a small lesion (arrow). Delayed phase image (a) shows persistent enhancement of the lesion that matches blood pool. In arterial phase (not shown in the figures), the lesion exhibited a rapid homogenous enhancement. Axial T_2 weighted image (b) shows increased signal intensity of the lesion typical of a flash filling haemangioma.
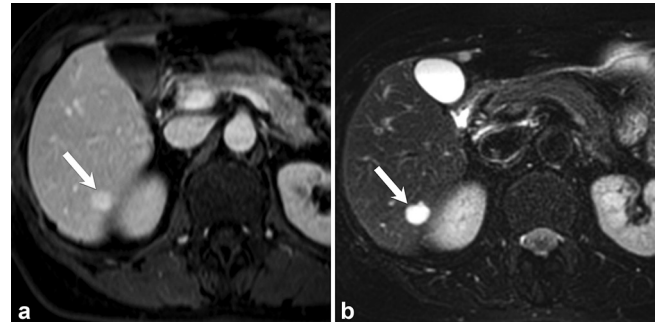
in the arterial phase, nodular regions of enhancement which are hyperintense on T_2 weighted images, decrease in size over time, capsular retraction and the presence of additional typical haemangiomas may suggest the possibility of a sclerosing haemangioma[10] (Figure 3).

Haemangiomatosis
Haemangiomatosis is a rare condition characterized by diffuse replacement of the liver by haemangiomatous lesions. Haemangiomatosis differs from multiple or giant haemangiomas in that the boundary of the lesions is poorly defined. Complications include spontaneous rupture, thrombocytopenia and consumptive coagulopathy (Kasabach–Merritt syndrome).[11] On ultrasound, this appears as a diffuse heterogeneous hyperechoic infiltrative mass with hypoechoic nodules.[11] On dynamic imaging, each lesion exhibits peripheral enhancement on the arterial phase with contrast retention on the delayed phase, which suggests its diagnosis (Figure 4). Differential diagnosis includes other vascular tumours such as epithelioid haemangioendothelioma (EHE) and angiosarcoma. Histology is generally required for confirmation.[12]

Figure 3. Sclerosing haemangioma, confirmed by histology: axial post-contrast T_1 weighted MR image in arterial (a) and delayed (b) phases, demonstrate a well-circumscribed lesion at the periphery of the right hepatic lobe (arrow) with rim enhancement on arterial phase and progressive incomplete filling on delayed phase with capsular retraction.
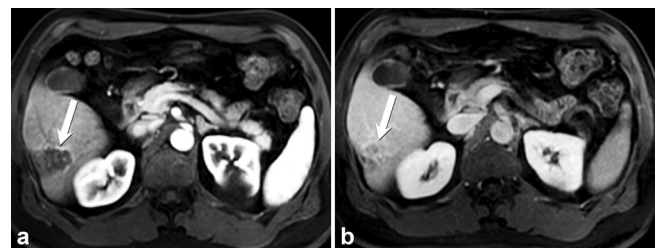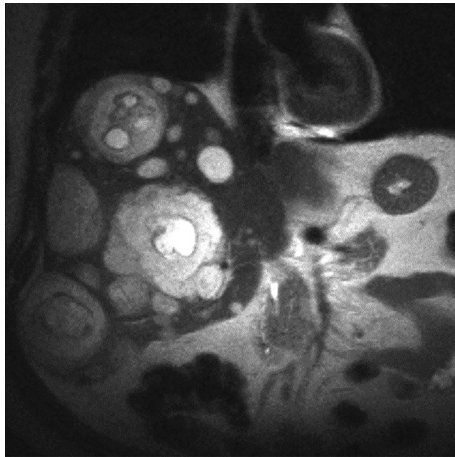
Figure 4. Haemangiomatosis. Coronal T2W HASTE demonstrates multiple haemangiomas in a patient with a known diagnosis of blue rubber bleb nevus syndrome.

Figure 5. Epithelioid haemangioendothelioma: contrast-enhanced CT in the arterial phase, showing multiple coalescent hypodense lesions with peripheral enhancement, more at the periphery of the right lobe; these were pathologically proven to represent EHE. EHE, epithelioid haemangioendothelioma.

Epithelioid haemangioendothelioma

Hepatic EHE is a rare tumour of vascular origin, akin to haemangioma and angiosarcoma. It is a low-grade malignant tumour that has an intermediate clinical outcome in between that of a benign hepatic cavernous haemangioma and malignant angiosarcoma. The vascular nature of the tumour is confirmed by positive staining for factor III related antigen and other endothelial cell markers (CD31, CD34).

Its peak incidence is between 30 and 50 years of age, and more commonly affects females.[13,14] Extrahepatic involvement at the time of diagnosis may be detected in up to 36% of patients, with metastatic spread to lungs, lymph nodes and peritoneum being the most common sites.[15] Recognition of EHE is important because it may be treated with surgical resection or transplantation even when metastatic disease is present.[16]

EHE usually manifests as multifocal tumours involving both lobes of the liver; only 13% are unifocal.[15] Tumours are composed of multiple solid nodules in a predominantly peripheral distribution, which coalesce as they enlarge, and result in capsular retraction. Tumour nodules have a hyperemic rim on the arterial phase which retains contrast on the venous phase.[13]

The mases are hypoechoic or heterogeneous on ultrasound. On CT, EHE presents as multiple peripherally located hypodense rim-enhancing tumours, resulting in capsular retraction in up to 25% of patients.[13] They can merge into larger confluent masses (Figure 5). A target pattern may be seen on contrast-enhanced CT or MR, characterized by a hypodense central zone, peripheral enhancement and a hypodense rim.[13,17–19] Imaging features may overlap with cholangiocarcinoma or multiple metastases. Pasquale et al reported a distinguishing feature in a series of 11 cases, in that none of them showed the globular enhancement pattern typical of haemangioma. EHE may also appear as a solitary subcapsular mass with minimal or rim-like enhancement at early phase and progressive centripetal fill-in enhancement during dynamic phase imaging, as seen in some haemangiomas.[20] EHE should be favoured over metastatic disease in cases

of multiple peripheral subcapsular lesions that demonstrate increased vascularity, and result in hypertrophy of the uninvolved liver.

Lipoma

Lipomas are rarely seen in the liver. Histologically, they consist of mature adipose tissue. On ultrasound, lipomas are well-circumscribed and homogeneously hyperechoic. They measure fat attenuation on CT with no enhancement on post-contrast imaging. On MRI, macroscopic adipose tissue demonstrates loss of signal on fat-saturated pulse sequences compared with non-fat-saturated pulse sequences. Microscopic adipose tissue demonstrates loss of signal on out-of-phase T_1 weighted images compared to in-phase images (Figure 6).

Perivascular epithelioid cell neoplasm (PEComa)

Perivascular epithelioid cell neoplasms (PEComa) are rare mesenchymal tumours composed of histologically and

Figure 6. Hepatic lipoma-gray-scale ultrasound demonstrates a well-circumscribed echogenic lesion with distal acoustic shadowing, consistent with lipoma.
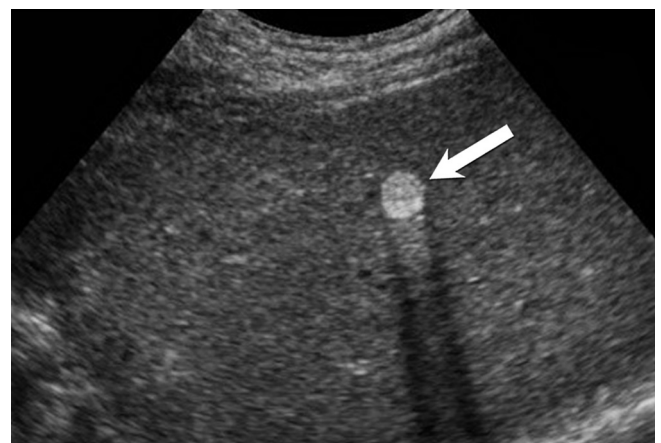
immunohistochemically distinctive "perivascular epithelioid cells", which are unusual cells with dual melanocytic and myxoid differentiation, typically in a perivascular distribution.[21] Although the majority are benign, they can show malignant features with local recurrence and distant metastases. It is important for radiologists to recognize the imaging findings of PEComas because treatment with mTOR inhibitors has shown promising results in malignant PEComas.[22]

The PEComa group of tumours includes classic angiomyolipoma (AML), epithelioid AML, clear-cell "sugar" tumours, lymphangioleiomyomatosis, clear-cell myomelanocytic tumour of the falciform ligament/ligamentum teres, and abdominopelvic sarcoma of PECs. AML is relatively specific to the tuberous sclerosis complex (TSC), presenting in 80% of patients with tuberous sclerosis and in less than 0.1% of the general population.[23] Hepatic AML is seen in about 30% tuberous sclerosis patients older than 9 years,[23] and nearly always seen concurrently with renal AML in TSC. Tumours comprised solely of PECs are distinguished from AML by names such as PEComa-NOS or simply PEComa. Malignant hepatic AML with metastases have been reported, but these tumours are usually large (greater than 15 cm).[24] Additional features associated with malignant AMLs are coagulative necrosis, rapid growth, metastases, and loss of CD117 expression.

Imaging features of hepatic PEComas vary due to their different degree of adipose tissue, vessels and smooth muscle. On ultrasound, PEComas are often hyperechoic similar to a haemangioma, but with blood flow within or at the periphery of the lesion. Lesions with increased smooth muscle components appear hypoechoic, whereas those with increased vascular components appear hyperechoic. CT and MRI usually demonstrate both the fat component and vessels[25] (Figure 7). In the presence of decreased fat content, distinguishing this tumour from other hypervascular tumours such as HCC may be difficult on CT and MRI since fatty metamorphosis can occur in HCC.[26] AMLs show a more prolonged enhancement in the portal phase, and on arterial phase about two-thirds demonstrate curved centralized vessels (whereas in HCC these vessels are more peripheral in location).[25] On MRI, these central vessels are depicted as flow voids, and vessels coursing within the fat strongly suggest AML[27] (Figure 7). When present, ancillary features such as an early draining vein connecting with tumour vessels or the absence of a capsule may be useful in differentiating lipid-poor hepatic AML/PEComas from hepatocellular carcinomas in a non-cirrhotic liver[28] (Figure 8).

Figure 7. Angiomyolipoma: axial non-contrast (a) and contrast-enhanced CT (b) demonstrate a large mass involving the left hepatic lobe with intralesional fat (arrow in a) and heterogeneous enhancement with prominent vessels (arrow in b).
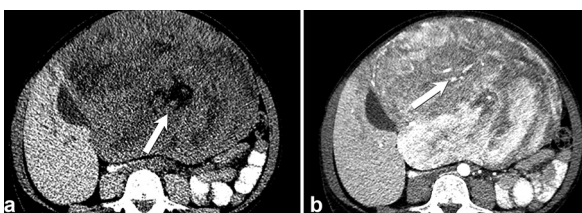

Figure 8. Malignant AML (PEComa): axial contrast-enhanced CT (a) demonstrates a well-circumscribed 2.6 cm mass with fat attenuation (arrow), initially reported as probably angiomyolipoma. Axial contrast-enhanced CT after 3 years (b) demonstrates stable size and appearance of the fatty mass. One year later, axial contrast-enhanced CT in the arterial (c) and delayed phase (d) demonstrated significant increase in size with the formation of a hypervascular mass with washout mimicking HCC, this was pathologically proven as a malignant AML (PEComa). AML, angiomyolipoma; HCC, hypervascular metastases; PEComa, perivascular epithelioid cell neoplasm.
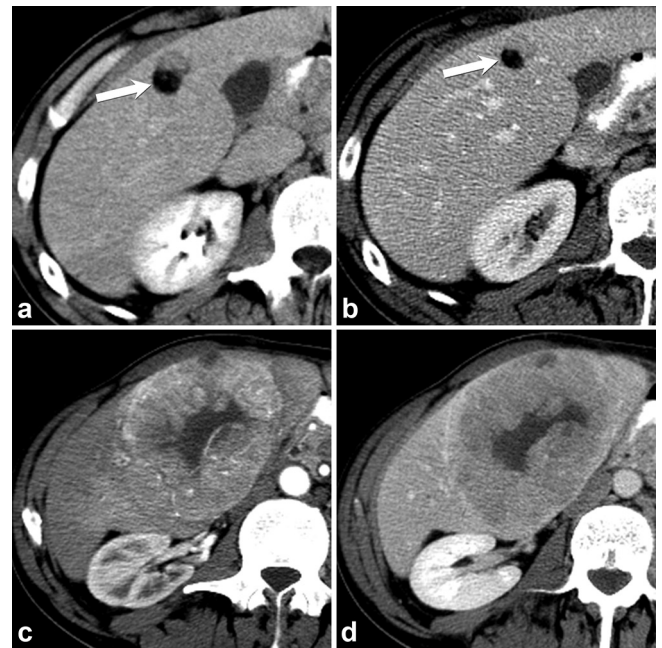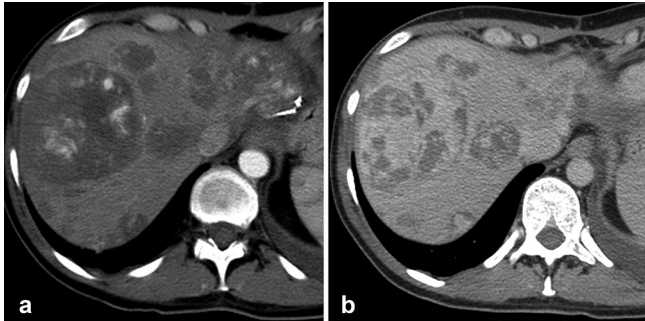

Angiosarcoma

Primary hepatic angiosarcoma is a rare but aggressive malignant vascular neoplasm. Most patients die within a year after diagnosis.[29] Prior exposure to thorotrast, arsenic and vinyl chloride have been implicated as causative factors. It is noted that up to 40% patients have underlying hepatic fibrosis and cirrhosis at diagnosis.[29] There are four reported cases of hepatic angiosarcoma arising from benign lesions such as haemangioendothelioma and haemangioma.[30,31] Multifocal involvement is typical, with at least 10 simultaneous lesions in the majority of patients.[29] Abnormal, pleomorphic, malignant endothelial cells are the hallmark of angiosarcoma, which can be rounded, polygonal or fusiform in shape.[32] Angiosarcoma typically expresses endothelial markers and vascular endothelial growth factor. Immunohistochemistry is therefore important in confirming the diagnosis.[32]

On CT wide variety of appearances may be seen in the late arterial phase, such as heterogeneous, multinodular, rim-like or a branching pattern of enhancement. The enhancing regions show progressive enhancement on the portal and delayed phases. Angiosarcoma classically does not exhibit washout, which is an important distinguishing feature from multifocal HCC.[29] Individual nodules are typically circumscribed and enhancing (Figure 9). Diffuse "flash-fill" and "reverse haemangioma" centrifugal enhancement patterns have also been reported.[29]

Figure 9. Angiosarcoma: axial contrast-enhanced CT in arterial (a) and venous (b) show multiple enhancing lesions compatible with angiosarcoma. The largest one exhibits enhancement pattern somewhat similar to haemangioma with delayed progressive enhancement—but with reversed centripetal pattern.

Figure 10. Inflammatory myofibroblastic tumour: coronal reformatted image of contrast-enhanced CT images in a 48-year-old patient with history of Epstein-Barr virus demonstrates multiple bilobar masses with predominantly peripheral enhancement in venous phase (arrows). Delayed phase image (not shown) shows central enhancement of the masses (arrows). Axial Fluorodeoxyglucose (FDG) PET scan (b) shows increased FDG uptake of the masses (arrows).

These multifocal tumours often contain haemorrhage resulting in heterogeneous appearance on MRI, with areas appearing hyperintense on T1WI and hypointense on T2WI. Extrahepatic metastases occur most commonly to the spleen, followed by peritoneum, pericardium, and lungs.[29]

Inflammatory myofibroblastic tumour

Inflammatory myofibroblastic tumour (IMT) is known by a variety of synonyms, such as inflammatory pseudotumour and plasma cell granuloma.[33] It should be considered in the differential diagnosis of a solid liver lesion in the setting of systemic symptoms (fever, fatigue, pain and weight loss), elevated inflammatory markers [leukocytosis, elevated erythrocyte sedimentation rate (ESR) and C-reactive protein (CRP)] and normal hepatic tumour markers (such as AFP, CA19-9).

Histologically, it consists of spindle cells, myofibroblasts, inflammatory cells and fibrous stroma. Although the exact cause is unknown, suggested causes include infection (*i.e.* EBV), vascular or an autoimmune process.[34]

The imaging features of IMT vary and are non-specific depending on the amount of fibrosis and cellular infiltration. It is solitary in more than 80% of the cases.[35] On ultrasound, it can be hypoechoic or hyperechoic with well-defined or infiltrative borders and often has increased vascularity on Doppler interrogation. Contrast-enhanced imaging shows various patterns of enhancement, including heterogeneous, homogeneous, septal enhancement, peripheral enhancement with delayed central filling, and lack of enhancement or central necrosis[35] (Figure 10). On MRI, it is usually T_1 hypointense and T_2 hyperintense with heterogeneous enhancement.[36] Since imaging findings are non-specific and malignancy is still a consideration, needle biopsy or resection is usually necessary. There are reported cases of shrinkage or disappearance of IMT with anti-inflammatory therapy.[37]

Solitary fibrous tumour

Solitary fibrous tumour (SFT) is a rare tumour composed of spindle cells and interspersed collagen. It rarely manifests in the liver; fewer than 100 cases have been reported, of which the

majority were benign and 16 cases demonstrated local recurrence or metastases.[38] Less than 5% of cases can have Doege-Potter syndrome which is defined as non-islet cell tumour hypoglycemia secondary to SFT, due to secretion of a prohormone form of insulin-like growth factor II.[39] At histopathology, SFT is typically composed of juxtaposed hyper- and hypocellular spindle cell proliferation, dense collagenous stroma and numerous thin-walled blood vessels with a staghorn configuration, a histologic hallmark of SFT.[40] SFT can be of the cellular or fibrous variant per the predominant histopathology and the imaging appearance varies accordingly.
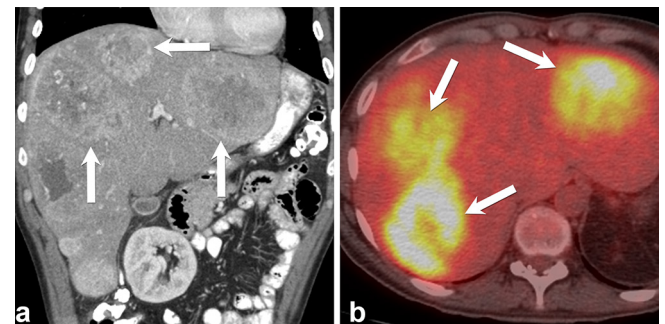
At imaging, it is typically a solitary large heterogeneous mass marked enhancement of the periphery, mimicking other tumours such as sclerosing haemangioma, sclerosing and fibrolamellar variants of hepatocellular carcinoma (Figure 11). The fibrous component may show progressive enhancement similar

Figure 11. Solitary fibrous tumour, pathologically proven: axial contrast-enhanced CT images show a large well defined hypodense lesion in the right lobe of the liver on precontrast CT (not shown) with marked peripheral enhancement.

to cholangiocarcinoma. It exhibits areas of low signal intensity on T_2 weighted images, corresponding to the fibrous component, which helps differentiate it from the other focal hepatic lesions, including cholangiocarcinoma, which is classically iso- or hyper-intense on T_2 weighted images.[41] Definitive diagnosis is based on typical histopathology and immunohistochemistry which include spindle cells arranged in a storiform pattern and immunohistochemical profile staining positive for CD34, vimentin, Bcl-2 and negative staining for actin, desmin and S-100.[42]

Leiomyoma

Leiomyoma is a benign smooth muscle tumour of mesenchymal origin. Only a few cases of primary hepatic leiomyoma have been reported.[43] It can develop in healthy individuals but association with immunodeficiency and Epstein-Barr virus has been observed.[44] Histologically, the tumour may need differentiation from gastrointestinal stromal tumours (GIST). On immunohistochemistry, leiomyomas are negative for the GIST marker CD117.[45] On imaging, it has well-defined margins rather than an infiltrative pattern. On dynamic contrast-enhanced CT and MRI, there is intense enhancement in the arterial phase which persists in the portal and delayed phases without evidence of washout.[46] Low signal on T_2 weighted images aids in differentiating it from a haemangioma[46] (Figure 12).

Leiomyosarcoma

Primary hepatic leiomyosarcoma is rare, and most cases are metastases from extrahepatic sites including the gastrointestinal tract, uterus, retroperitoneum and lung.[47] Serum markers such as alpha fetoprotein tend to be normal.

Pathology shows infiltrates of spindle-shaped cells with hyperchromatic nuclei. Immunohistochemistry is positive for desmin, vimentin, and SMA, but negative for keratin, S-100 protein, and neuron-specific enolase. Needle biopsy will allow for definitive diagnosis.[48]

CT classically demonstrates a large, marginated, heterogeneous hypodense mass with internal and peripheral enhancement (Figure 13). A cystic mass with an enhanced thickened wall has also been reported, which may mimic an abscess or

Figure 12. Leiomyoma: axial contrast-enhanced axial CT (a) shows a well-circumscribed oval-shaped enhancing mass within the left hepatic lobe. Axial T_2 weighted (b) image demonstrates peripheral low signal intensity and central hyperintensity on T_2 weighted images. This demonstrated a low signal intensity on T_1 weighted image (not shown). This mass was pathologically proven to represent a benign smooth muscle tumour (leiomyoma).
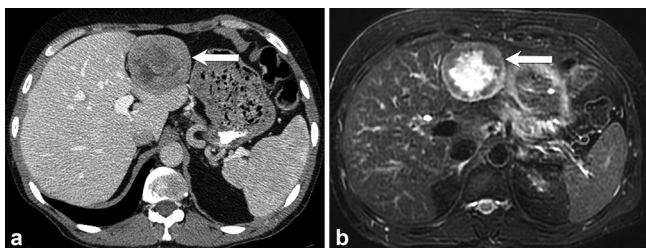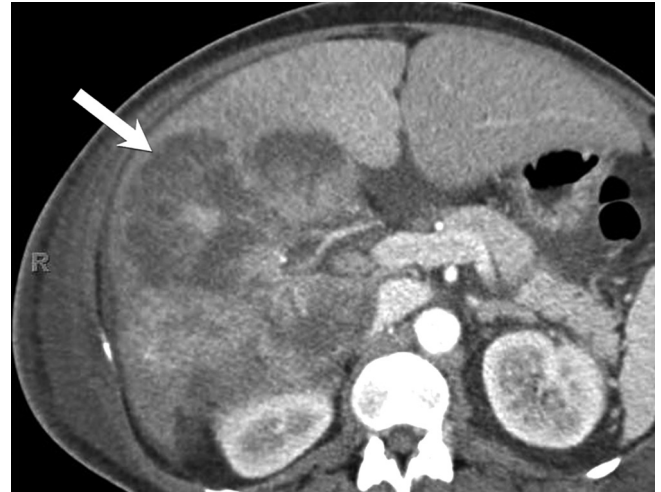

Figure 13. Leiomyosarcoma: axial contrast-enhanced CT showing a large heterogeneously enhancing predominantly hypoattenuating mass (arrow) occupying the right hepatic lobe. This was pathologically proven to represent leiomyosarcoma.

hydatid cyst.[49] On MRI, it shows homogenous or heterogeneous hypointensity on T_1 weighted images, and hyperintensity on T_2 weighted images. Lack of enhancement in the arterial and venous phases followed by marked enhancement on the delayed phase has been reported and may be a useful finding.[50]

Kaposi sarcoma

Kaposi sarcoma is a low-grade malignancy associated with human herpes virus 8 (HHV-8). It is the most common intrahepatic neoplasm in patients with AIDS, found in 34% of AIDS patients at autopsy.[51] It is also seen in solid organ transplant recipients, although rare.[52]

It is typically found in the perivascular areas around the peripheral portal branches. It consists of multiple nodules and shows diffuse macrovacuolar steatosis, with perinodular tissue featuring small vascular structures. By immunohistochemical detection of endothelial cell markers such as CD31 and CD34, Kaposi sarcoma can be differentiated from non-vascular spindle cell neoplasms. Detection of HHV-8 LNA-1 and D2-40 is useful to differentiate Kaposi sarcoma from other vascular tumours.[53]

On ultrasound, the liver appears heterogeneous with multiple hyperechoic nodules and periportal hyperechogenecity.[54] CT shows hypoattenuating nodules which exhibit delayed enhancement (Figure 14). MRI shows nodules which are hyperintense on T_1 in-phase and hypointense on T_1 out-of-phase due to the presence of lipid.[51]

Mesenchymal hamartoma

Mesenchymal hamartoma (MH) is the second most common benign liver tumour in children younger than 5 years. Less than 20 cases have been reported in adults.[55] Although there are reports of its spontaneous regression, it can potentially progress to an aggressive malignant undifferentiated embryonal sarcoma (UES). Therefore, surgical resection is the most favoured

Figure 14. Kaposi's sarcoma: axial contrast-enhanced CT (a and c) and fused PET/CT (b and d) images demonstrate a small hypoattenuating lesion within segment 7 of the liver (arrows in a and b) and an enlarged right inguinal lymph node (arrows in c and d). Both the liver lesion and inguinal lymph node were biopsied and found to represent Kaposi's sarcoma.
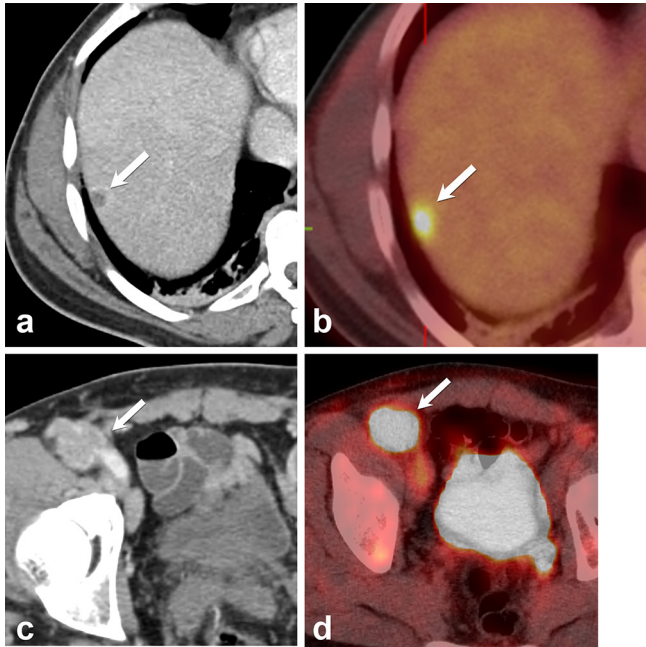
treatment option.[55] A continuum between MH and UES is considered since they share several common histopathologic, immunohistochemical, and cytogenetic features.[56]

MH classically consists of variable-sized cysts. Its appearance can vary from predominantly cystic to predominantly mesenchymal. Its mesenchymal components show stellate cells in a loose mucopolysaccharide matrix surrounded by vessels and bile ducts.[56]

On ultrasound, the classic appearance is a complex cystic mass with internal septations. A complex cystic mass with septal and solid stromal enhancement can be seen on CT and MRI[57] (Figure 15), and high signal intensity of cystic components on T_2 weighted images, with variable signal intensity on T_1 weighted images due to varying internal proteinaceous components.

Figure 15. Mesenchymal hamartoma: gray scale US (a) shows complex cystic mass with solid component. Contrast CT image (b) shows a complex cystic appearing right hepatic mass, which was surgically resected and found to represent mesenchymal hamartoma.
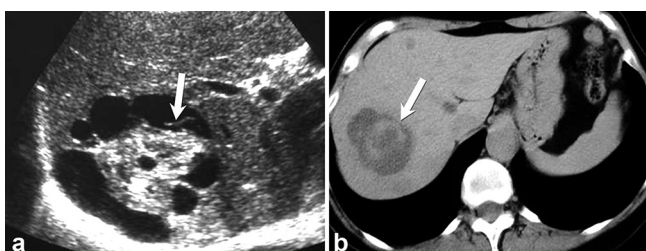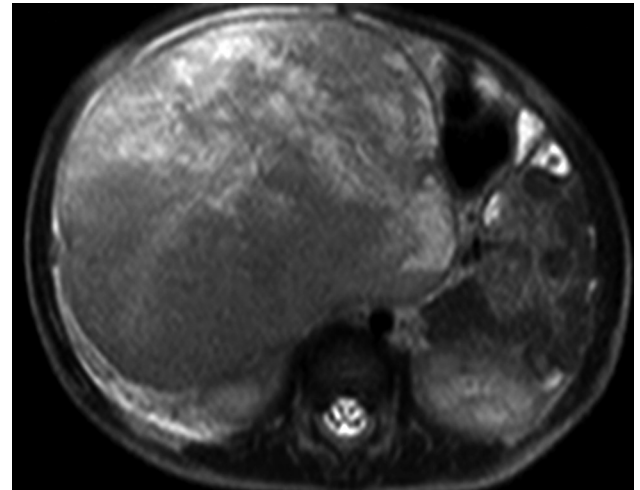

Figure 16. Undifferentiated embryonal sarcoma: axial T_2 weighted image shows a large heterogeneous mass occupying the left and part of the right lobe of the liver exhibiting increased signal intensity with several cystic areas. Axial contrast-enhanced CT (not shown) demonstrated predominant hypoattenuation of the mass. This was pathologically proven to be UES. UES, undifferentiated embryonal sarcoma.

Undifferentiated embryonal sarcoma

UES is a rare malignant mesenchymal tumour more common in children, although a few cases of adult UES have been reported.[58] It is the third most common primary malignant tumour of the liver in childhood, after hepatoblastoma and hepatocellular carcinoma.[59]

UES consists of sarcomatous cells associated with a myxoid stroma. A definitive pathological diagnosis of UES is based on immunohistochemical analysis that is positive for CD56, CD68, vimentin and desmin. It is negative for hepatocyte paraffin 1 (aka hep par 1) and myogenin, which differentiates UES from hepatoblastoma, HCC, and rhabdomyosarcoma (RMS), respectively.[60]

Discrepancy between its predominantly solid-like appearance on US and cyst-like appearance on CT has been the classical description of UES.[61] This may be attributable to varying myxoid content, which is hyperechoic on ultrasound and cystic

Figure 17. Rhabdomyosarcoma: axial contrast-enhanced CT (a) showing a large predominantly hypoattenuating mass occupying the left and part of the right lobe of the liver. Coronal T_2 weighted images (b) demonstrate the fluid-like signal intensity of the mass. This was pathologically proven as Rhabdomyosarcoma.

on CT. The solid components and septations show progressive enhancement at dynamic contrast CT/MRI (Figure 16). Gabor et al described the presence of serpentine vessels within the tumour on arterial phase in 10 out of 15 cases, which would be helpful in the diagnosis of UES when a cystic lesion with internal vessels is detected on CT.[58] It is associated with a risk of spontaneous rupture which can cause hemoperitoneum and peritoneal seeding.[62] Metastases to the lungs, pleura and peritoneum have been described.[63,64]
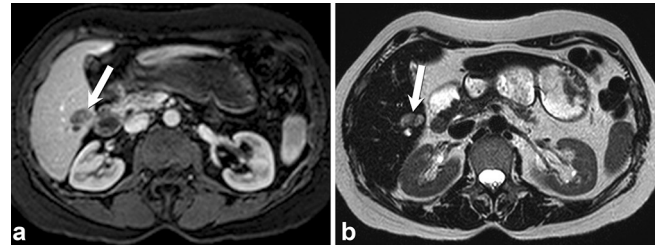
Rhabdomyosarcoma

RMS is a highly malignant tumour which may rarely arise in the biliary tree. The mean age of presentation is 3 years and it is rare after the first decade.[65] Most patients present with jaundice and fever, mimicking hepatitis.[61] It commonly arises in the extrahepatic biliary tree, so the mass is usually adjacent to the porta hepatis and may grow into intrahepatic biliary system, invading the liver.[66] It is histologically identical to sarcoma botryoides, commonly arising from the bladder or vagina of children. It therefore is at risk of being misclassified as UES. Distinguishing the two is important because treatment differs. Positive myogenin in RMS on immunohistochemistry helps in distinguishing it from UES.[67]

Ultrasound usually demonstrates biliary dilation with an intraluminal mass, often with associated displacement of the portal vein without intraluminal thrombus. CT shows a intraductal mass with or without biliary dilatation.[68] Hypodense and heterogeneous tumour patterns can be seen. The pattern of enhancement also varies and may show different patterns including intense, globular, mild or even no enhancement. On MRI, it is typically a predominantly fluid-intensity mass which is T_1 hypointense and T_2 hyperintense[69](Figure 17). Although many types of masses may cause biliary obstruction in children, only embryonal RMS arises from the biliary tree.[66]

Figure 18. Metastatic GIST: axial contrast-enhanced CT shows multiple hypoattenuating liver metastases (arrows) in a 57-year-old male patient with GIST. The lesions exhibit peripheral enhancement and central fluid attenuation. GIST, gastrointestinalstromal tumours.

Figure 19. Metastatic leiomyosarcoma: axial contrast-enhanced T_1 weighted image (a) demonstrates heterogeneously enhancing mass (arrow) in segment V of the liver, which appears hypointense relative to the surrounding parenchyma. Axial T_2 weighted image (b) demonstrates increased signal intensity of the mass. Surgical resection and pathological evaluation confirmed the diagnosis of metastasis from small bowel leiomyosarcoma.

Secondary mesenchymal tumours

Mesenchymal tumours may metastasize to the liver. The liver is a common site of metastases from leiomyosarcoma and malignant GIST tumours.[69] Metastatic GIST tumours have imaging characteristics similar to their primary tumour site. They are usually hyperattenuating/hyperintense, enhancing masses with necrosis, haemorrhage or cystic degeneration. Tumour vessels may be seen within the tumour[70] (Figure 18).

The most common MRI appearance of metastatic leiomyosarcoma is a well-defined homogenous mass with marked hyperintensity on T_2 weighted images, similar to a hepatic haemangioma.[71] On post-contrast imaging, it usually demonstrates peripheral rim enhancement and central necrotic areas[72] (Figure 19).

Myxoid liposarcoma commonly metastasizes to the retroperitoneum, bone, and soft tissues. About one-third metastases occur in the liver. On CT, this appears as multifocal, hypodense lesions with minimal peripheral enhancement.[73] Fat may or may not be identified on imaging, depending on tumour differentiation[73] (Figure 20).

CONCLUSION

Mesenchymal tumours of the liver vary widely in their imaging appearances due to the different components that comprise

Figure 20. Metastatic liposarcoma: axial contrast-enhanced CT shows multiple liver metastases containing fat (arrows in a) and a large heterogeneously enhancing predominantly mesenteric mass containing macroscopic fat (arrow in b), consistent with metastatic liposarcoma.
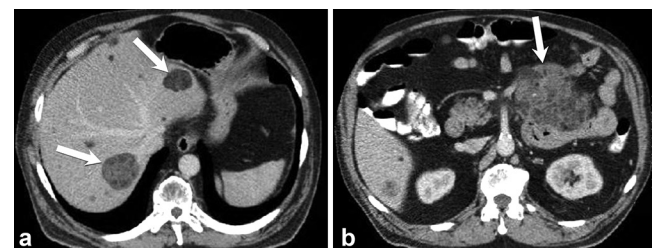
each of the various tumour types. They may be indistinguishable from other benign and malignant liver tumours, and the diagnosis at times may only be reached after pathologic confirmation with biopsy or resection. However, many typical clinical and imaging findings of mesenchymal tumours have been described. Knowledge of these distinguishing features will aid in guiding the radiologic diagnosis and correct patient management.

REFERENCES

1. Kaltenbach TE, Engler P, Kratzer W, Oeztuerk S, Seufferlein T, Haenle MM, et al. Prevalence of benign focal liver lesions: ultrasound investigation of 45,319 hospital patients. *Abdom Radiol* 2016; **41**: 25–32. doi: https://doi.org/10.1007/s00261-015-0605-7

2. Mocchegiani F, Vincenzi P, Coletta M, Agostini A, Marzioni M, Baroni GS, et al. Prevalence and clinical outcome of hepatic haemangioma with specific reference to the risk of rupture: a large retrospective cross-sectional study. *Dig Liver Dis* 2016; **48**: 309–14. doi: https://doi.org/10.1016/j.dld.2015.09.016

3. Quinn SF, Benjamin GG. Hepatic cavernous hemangiomas: simple diagnostic sign with dynamic bolus CT. *Radiology* 1992; **182**: 545–8. doi: https://doi.org/10.1148/radiology.182.2.1732978

4. Mitchell DG, Saini S, Weinreb J, De Lange EE, Runge VM, Kuhlman JE, et al. Hepatic metastases and cavernous hemangiomas: distinction with standard- and triple-dose gadoteridol-enhanced MR imaging. *Radiology* 1994; **193**: 49–57. doi: https://doi.org/10.1148/radiology.193.1.8090921

5. Semelka RC, Sofka CM. Hepatic hemangiomas. *Magn Reson Imaging Clin N Am* 1997; **5**: 241–53.

6. McFarland EG, Mayo-Smith WW, Saini S, Hahn PF, Goldberg MA, Lee MJ, et al. Hepatic hemangiomas and malignant tumors: improved differentiation with heavily T2-weighted conventional spin-echo MR imaging. *Radiology* 1994; **193**: 43–7. doi: https://doi.org/10.1148/radiology.193.1.8090920

7. Danet IM, Semelka RC, Braga L, Armao D, Woosley JT. Giant hemangioma of the liver: MR imaging characteristics in 24 patients. *Magn Reson Imaging* 2003; **21**: 95–101. doi: https://doi.org/10.1016/S0730-725X(02)00641-0

8. Hanafusa K, Ohashi I, Himeno Y, Suzuki S, Shibuya H. Hepatic hemangioma: findings with two-phase CT. *Radiology* 1995; **196**: 465–9. doi: https://doi.org/10.1148/radiology.196.2.7617862

9. Kim T, Federle MP, Baron RL, Peterson MS, Kawamori Y. Discrimination of small hepatic hemangiomas from hypervascular malignant tumors smaller than 3 cm with three-phase helical CT. *Radiology* 2001; **219**: 699–706. doi: https://doi.org/10.1148/radiology.219.3.r01jn45699

10. Doyle DJ, Khalili K, Guindi M, Atri M. Imaging features of sclerosed hemangioma. *AJR Am J Roentgenol* 2007; **189**: 67–72. doi: https://doi.org/10.2214/AJR.06.1076

11. Maeda E, Akahane M, Watadani T, Yoshioka N, Goto A, Sugawara Y, et al. Isolated hepatic hemangiomatosis in adults: report of two cases and review of the literature. *Eur J Radiol Extra* 2007; **61**: 9–14. doi: https://doi.org/10.1016/j.ejrex.2006.10.007

12. Chung EM, Lattin GE, Cube R, Lewis RB, Marichal-Hernández C, Shawhan R, et al. From the archives of the AFIP: pediatric liver masses: radiologic-pathologic correlation part 2. Malignant tumors. *Radiographics* 2011; **31**: 483–507. doi: https://doi.org/10.1148/rg.312105201

13. Miller WJ, Dodd GD, 3rd, Federle MP, Baron RL. Epithelioid hemangioendothelioma of the liver: imaging findings with pathologic correlation. *AJR Am J Roentgenol* 1992; **159**: 53–7. doi: https://doi.org/10.2214/ajr.159.1.1302463

14. Da Ines D, Petitcolin V, Joubert-Zakeyh J, Demeocq F, Garcier JM. Epithelioid hemangioendothelioma of the liver with metastatic coeliac lymph nodes in an 11-year-old boy. *Pediatr Radiol* 2010; **40**: 1293–6. doi: https://doi.org/10.1007/s00247-009-1532-y

15. Mehrabi A, Kashfi A, Fonouni H, Schemmer P, Schmied BM, Hallscheidt P, et al. Primary malignant hepatic epithelioid hemangioendothelioma: a comprehensive review of the literature with emphasis on the surgical therapy. *Cancer* 2006; **107**: 2108–21. doi: https://doi.org/10.1002/cncr.22225

16. Madariaga JR, Marino IR, Karavias DD, Nalesnik MA, Doyle HR, Iwatsuki S, et al. Long-term results after liver transplantation for primary hepatic epithelioid hemangioendothelioma. *Ann Surg Oncol* 1995; **2**: 483–7. doi: https://doi.org/10.1007/BF02307080

17. Economopoulos N, Kelekis NL, Argentos S, Tsompanlioti C, Patapis P, Nikolaou I, et al. Bright-dark ring sign in MR imaging of hepatic epithelioid hemangioendothelioma. *J Magn Reson Imaging* 2008; **27**: 908–12. doi: https://doi.org/10.1002/jmri.21052

18. Paolantonio P, Laghi A, Vanzulli A, Grazioli L, Morana G, Ragozzino A, et al. MRI of hepatic epithelioid hemangioendothelioma (HEH). *J Magn Reson Imaging* 2014; **40**: 552–8. doi: https://doi.org/10.1002/jmri.24391

19. Kehagias DT, Moulopoulos LA, Antoniou A, Psychogios V, Vourtsi A, Vlahos LJ, et al. Hepatic epithelioid hemangioendothelioma: MR imaging findings. *Hepatogastroenterology* 2000; **47**: 1711–3.

20. Kim EH, Rha SE, Lee YJ, Yoo I, Jung ES, Byun JY, et al. CT and MR imaging findings of hepatic epithelioid hemangioendotheliomas: emphasis on single nodular type. *Abdom Imaging* 2015; **40**: 500–9. doi: https://doi.org/10.1007/s00261-014-0229-3

21. Folpe AL, Kwiatkowski DJ. Perivascular epithelioid cell neoplasms: pathology and pathogenesis. *Hum Pathol* 2010; **41**: 1–15. doi: https://doi.org/10.1016/j.humpath.2009.05.011

22. Wagner AJ, Malinowska-Kolodziej I, Morgan JA, Qin W, Fletcher CD, Vena N, et al. Clinical activity of mTOR inhibition with sirolimus in malignant perivascular epithelioid cell tumors: targeting the pathogenic activation of mTORC1 in tumors. *J Clin Oncol* 2010; **28**: 835–40. doi: https://doi.org/10.1200/JCO.2009.25.2981

23. Northrup H, Krueger DA, Roberds S, International Tuberous Sclerosis Complex Consensus Group. Tuberous sclerosis complex diagnostic criteria update: recommendations of the 2012 International Tuberous Sclerosis complex Consensus Conference. *Pediatr Neurol* 2013; **49**: 243–54. doi: https://doi.org/10.1016/j.pediatrneurol.2013.08.001

24. O'Malley ME, Chawla TP, Lavelle LP, Cleary S, Fischer S. Primary perivascular epithelioid cell tumors of the liver: CT/MRI findings and clinical outcomes. *Abdom*

Radiol 2017; **42**: 1705–12. doi: https://doi.org/10.1007/s00261-017-1074-y

25. Yan F, Zeng M, Zhou K, Shi W, Zheng W, Da R, et al. Hepatic angiomyolipoma: various appearances on two-phase contrast scanning of spiral CT. *Eur J Radiol* 2002; **41**: 12–18. doi: https://doi.org/10.1016/S0720-048X(01)00392-8

26. Yoshikawa J, Matsui O, Takashima T, Ida M, Takanaka T, Kawamura I, et al. Fatty metamorphosis in hepatocellular carcinoma: radiologic features in 10 cases. *AJR Am J Roentgenol* 1988; **151**: 717–20. doi: https://doi.org/10.2214/ajr.151.4.717

27. Yan F, Li R, Shen J, Zeng M, Zhou K, Fan J, et al. Hepatic angiomyolipoma: MRI findings. *Eur J Radiol Extra* 2003; **45**: 101–8. doi: https://doi.org/10.1016/S1571-4675(03)00025-7

28. Jeon TY, Kim SH, Lim HK, Lee WJ. Assessment of triple-phase CT findings for the differentiation of fat-deficient hepatic angiomyolipoma from hepatocellular carcinoma in non-cirrhotic liver. *Eur J Radiol* 2010; **73**: 601–6. doi: https://doi.org/10.1016/j.ejrad.2009.01.010

29. Pickhardt PJ, Kitchin D, Lubner MG, Ganeshan DM, Bhalla S, Covey AM, et al. Primary hepatic angiosarcoma: multi-institutional comprehensive cancer centre review of multiphasic CT and MR imaging in 35 patients. *Eur Radiol* 2015; **25**: 315–22. doi: https://doi.org/10.1007/s00330-014-3442-0

30. Kamath SM, Mysorekar VV, Kadamba P. Hepatic angiosarcoma developing in an infantile hemangioendothelioma: a rare case report. *J Cancer Res Ther* 2015; **11**: 1022. doi: https://doi.org/10.4103/0973-1482.146132

31. Rossi S, Fletcher CD. Angiosarcoma arising in hemangioma/vascular malformation: report of four cases and review of the literature. *Am J Surg Pathol* 2002; **26**: 1319–29.

32. Young RJ, Brown NJ, Reed MW, Hughes D, Woll PJ. Angiosarcoma. *Lancet Oncol* 2010; **11**: 983–91. doi: https://doi.org/10.1016/S1470-2045(10)70023-1

33. Tang L, Lai EC, Cong WM, Li AJ, Fu SY, Pan ZY, et al. Inflammatory myofibroblastic tumor of the liver: a cohort study. *World J Surg* 2010; **34**: 309–13. doi: https://doi.org/10.1007/s00268-009-0330-x

34. Horiuchi R, Uchida T, Kojima T, Shikata T. Inflammatory pseudotumor of the liver. Clinicopathologic study and review of the literature. *Cancer* 1990; **65**: 1583–90. doi: https://doi.org/10.1002/1097-0142(19900401)65:7<1583::AID-CNCR2820650722>3.0.CO;2-L

35. Nam KJ, Kang HK, Lim JH. Inflammatory pseudotumor of the liver: CT and sonographic findings. *Am J Roentgenol* 1996; **167**: 485–7. doi: https://doi.org/10.2214/ajr.167.2.8686633

36. Yan FH, Zhou KR, Jiang YP, Shi WB. Inflammatory pseudotumor of the liver: 13 cases of MRI findings. *World J Gastroenterol* 2001; **7**: 422. doi: https://doi.org/10.3748/wjg.v7.i3.422

37. Yamaguchi J, Sakamoto Y, Sano T, Shimada K, Kosuge T. Spontaneous regression of inflammatory pseudotumor of the liver: report of three cases. *Surg Today* 2007; **37**: 525–9. doi: https://doi.org/10.1007/s00595-006-3433-0

38. Chen N, Slater K. Solitary fibrous tumour of the liver—report on metastasis and local recurrence of a malignant case and review of literature. *World J Surg Oncol* 2017; **15**: 27. doi: https://doi.org/10.1186/s12957-017-1102-y

39. Schutt RC, Gordon TA, Bhabhra R, Cathro HP, Cook SL, McCartney CR, et al. Doege-Potter syndrome presenting with hypoinsulinemic hypoglycemia in a patient with a malignant extrapleural solitary fibrous tumor: a case report. *J Med Case Rep* 2013; **7**: 11. doi: https://doi.org/10.1186/1752-1947-7-11

40. Ide F, Obara K, Mishima K, Saito I, Kusama K. Ultrastructural spectrum of solitary fibrous tumor: a unique perivascular tumor with alternative lines of differentiation. *Virchows Arch* 2005; **446**: 646–52. doi: https://doi.org/10.1007/s00428-005-1261-z

41. Shanbhogue AK, Prasad SR, Takahashi N, Vikram R, Zaheer A, Sandrasegaran K, et al. Somatic and visceral solitary fibrous tumors in the abdomen and pelvis: cross-sectional imaging spectrum. *Radiographics* 2011; **31**: 393–408. doi: https://doi.org/10.1148/rg.312105080

42. Fuksbrumer MS, Klimstra D, Panicek DM. Solitary fibrous tumor of the liver. *Am J Roentgenol* 2000; **175**: 1683–7. doi: https://doi.org/10.2214/ajr.175.6.1751683

43. Vyas S, Psica A, Watkins J, Yu D, Davidson B. Primary hepatic leiomyoma: unusual cause of an intrahepatic mass. *Ann Transl Med* 2015; **3**: 73. doi: https://doi.org/10.3978/j.issn.2305-5839.2015.03.40

44. Davidoff AM, Hebra A, Clark BJ 3rd, Tomaszewski JE, Montone KT, Ruchelli E, et al. Epstein-Barr virus-associated hepatic smooth muscle neoplasm in a cardiac transplant recipient. *Transplantation* 1996; **61**: 515–7. doi: https://doi.org/10.1097/00007890-199602150-00036

45. Sarlomo-Rikala M, Kovatich AJ, Barusevicius A, Miettinen M. CD117: a sensitive marker for gastrointestinal stromal tumors that is more specific than CD34. *Mod Pathol* 1998; **11**: 728–34.

46. Marin D, Catalano C, Rossi M, Guerrisi A, Di Martino M, Berloco P, et al. Gadobenate dimeglumine-enhanced magnetic resonance imaging of primary leiomyoma of the liver. *J Magn Reson Imaging* 2008; **28**: 755–8. doi: https://doi.org/10.1002/jmri.21519

47. Cioffi U, Quattrone P, De Simone M, Bonavina L, Segalin A, Masini T, et al. Primary multiple epithelioid leiomyosarcoma of the liver. *Hepatogastroenterology* 1996; **43**: 1603–5.

48. Smith MB, Silverman JF, Raab SS, Towell BD, Geisinger KR. Fine-needle aspiration cytology of hepatic leiomyosarcoma. *Diagn Cytopathol* 1994; **11**: 321–7. doi: https://doi.org/10.1002/dc.2840110403

49. Shivathirthan N, Kita J, Iso Y, Hachiya H, Kyunghwa P, Sawada T, et al. Primary hepatic leiomyosarcoma: case report and literature review. *World J Gastrointest Oncol* 2011; **3**: 148–52. doi: https://doi.org/10.4251/wjgo.v3.i10.148

50. Soyer P, Blanc F, Vissuzaine C, Marmuse JP, Menu Y. Primary leiomyosarcoma of the liver MR findings. *Clin Imaging* 1996; **20**: 273–5. doi: https://doi.org/10.1016/0899-7071(95)00043-7

51. Tacconi D, Vergori A, Lapini L, Magnolfi A, Carnevali A, Caremani M, et al. Hepatic Kaposi's sarcoma in a patient affected by AIDS: correlation between histology and imaging. *J Ultrasound* 2012; **15**: 215–9. doi: https://doi.org/10.1016/j.jus.2012.10.004

52. Gupta S, Ghuman SS, Buxi TBS, Sudarsan H, Sethi S, Yadav AK, et al. Imaging of Kaposi sarcoma in a transplanted liver: a rare case report. *The Egyptian Journal of Radiology and Nuclear Medicine* 2015; **46**: 335–8. doi: https://doi.org/10.1016/j.ejrnm.2015.02.007

53. Lee KB, Lee HS, Lee HE, et al. Immunohistochemical characteristics of Kaposi sarcoma and its mimicries. *J Pathol Transl Med* 2006; **40**: 361–7.

54. Restrepo CS, Martínez S, Lemos JA, Carrillo JA, Lemos DF, Ojeda P, et al. Imaging manifestations of Kaposi sarcoma. *Radiographics* 2006; **26**: 1169–85. doi: https://doi.org/10.1148/rg.264055129

55. Stringer MD, Alizai NK. Mesenchymal hamartoma of the liver: a systematic review. *J Pediatr Surg* 2005; **40**: 1681–90. doi: https://doi.org/10.1016/j.jpedsurg.2005.07.052

56. Chung EM, Cube R, Lewis RB, Conran RM. From the archives of the AFIP: pediatric liver masses: radiologic-pathologic correlation part 1. Benign tumors. *Radiographics* 2010;

30: 801–26. doi: https://doi.org/10.1148/rg.303095173

57. Stanley P, Hall TR, Woolley MM, Diament MJ, Gilsanz V, Miller JH, et al. Mesenchymal hamartomas of the liver in childhood: sonographic and CT findings. *AJR Am J Roentgenol* 1986; **147**: 1035–9. doi: https://doi.org/10.2214/ajr.147.5.1035

58. Gabor F, Franchi-Abella S, Merli L, Adamsbaum C, Pariente D. Imaging features of undifferentiated embryonal sarcoma of the liver: a series of 15 children. *Pediatr Radiol* 2016; **46**: 1694–704. doi: https://doi.org/10.1007/s00247-016-3670-3

59. Chung EM, Lattin GE, Cube R, Lewis RB, Marichal-Hernández C, Shawhan R, et al. From the archives of the AFIP: pediatric liver masses: radiologic-pathologic correlation. part 2. Malignant tumors. *Radiographics* 2011; **31**: 483–507. doi: https://doi.org/10.1148/rg.312105201

60. Putra J, Ornvold K. Undifferentiated embryonal sarcoma of the liver: a concise review. *Arch Pathol Lab Med* 2015; **139**: 269–73. doi: https://doi.org/10.5858/arpa.2013-0463-RS

61. Stocker JT. Hepatic tumors in children. *Clin Liver Dis* 2001; **5**: 259–81. doi: https://doi.org/10.1016/S1089-3261(05)70163-X

62. Qiu LL, Yu RS, Chen Y, Zhang Q. Sarcomas of abdominal organs: computed tomography and magnetic resonance imaging findings. *Semin Ultrasound CT MR* 2011; **32**: 405–21.

doi: https://doi.org/10.1053/j.sult.2011.04.003

63. Chung EM, Lattin GE, Cube R, Lewis RB, Marichal-Hernández C, Shawhan R, et al. From the archives of the AFIP: pediatric liver masses: radiologic-pathologic correlation part 2. Malignant tumors. *Radiographics* 2011; **31**: 483–507. doi: https://doi.org/10.1148/rg.312105201

64. Yu R-S, Chen Y, Jiang B, Wang L-H, Xu X-F, et al. Primary hepatic sarcomas: CT findings. *Eur Radiol* 2008; **18**: 2196–205. doi: https://doi.org/10.1007/s00330-008-0997-7

65. Ruymann FB, Raney RB Jr, Crist WM, Lawrence W, Lindberg RD, Soule EH. Rhabdomyosarcoma of the biliary tree in childhood. A report from the Intergroup Rhabdomyosarcoma Study. *Cancer* 1985; **56**: 575–81.

66. Donnelly LF, Bisset GS 3rd, Frush DP. Diagnosis please. Case 2: embryonal rhabdomyosarcoma of the biliary tree. *Radiology* 1998; **208**: 621–3. doi: https://doi.org/10.1148/radiology.208.3.9722837

67. Nicol K, Savell V, Moore J, Teot L, Spunt SL, Qualman S, et al. Distinguishing undifferentiated embryonal sarcoma of the liver from biliary tract rhabdomyosarcoma: a children's oncology group study. *Pediatr Dev Pathol* 2007; **10**: 89–97. doi: https://doi.org/10.2350/06-03-0068.1

68. Roebuck DJ, Yang WT, Lam WW, Stanley P. Hepatobiliary rhabdomyosarcoma in

children: diagnostic radiology. *Pediatr Radiol* 1998; **28**: 101–8. doi: https://doi.org/10.1007/s002470050305

69. Lang H, Nussbaum KT, Kaudel P, Frühauf N, Flemming P, Raab R. Hepatic metastases from leiomyosarcoma: a single-center experience with 34 liver resections during a 15-year period. *Ann Surg* 2000; **231**: 500–5. doi: https://doi.org/10.1097/00000658-200004000-00007

70. Hong X, Choi H, Loyer EM, Benjamin RS, Trent JC, Charnsangavej C, et al. Gastrointestinal Stromal tumor: role of CT in diagnosis and in response evaluation and surveillance after treatment with imatinib. *Radiographics* 2006; **26**: 481–95. doi: https://doi.org/10.1148/rg.262055097

71. Soyer P, Riopel M, Bluemke DA, Scherrer A. Hepatic metastases from leiomyosarcoma: MR features with histopathologic correlation. *Abdom Imaging* 1997; **22**: 67–71. doi: https://doi.org/10.1007/s002619900142

72. McLeod AJ, Zornoza J, Shirkhoda A. Leiomyosarcoma: computed tomographic findings. *Radiology* 1984; **152**: 133–6. doi: https://doi.org/10.1148/radiology.152.1.6729102

73. Sheah K, Ouellette HA, Torriani M, Nielsen GP, Kattapuram S, Bredella MA, et al. Metastatic myxoid liposarcomas: imaging and histopathologic findings. *Skeletal Radiol* 2008; **37**: 251–8. doi: https://doi.org/10.1007/s00256-007-0424-1